

Content from this work may be used under the terms of the CC BY 3.0 licence (© 2019). Any distribution of this work must maintain attribution to the author(s), title of the work, publisher, and DOI.

AN APPLICATION OF MACHINE LEARNING FOR THE ANALYSIS OF TEMPERATURE RISE ON THE PRODUCTION TARGET IN HADRON EXPERIMENTAL FACILITY AT J-PARC

K. Agari[†], H. Akiyama, Y. Morino, Y. Sato, A. Toyoda, KEK, Ibaraki, Japan

Abstract

Hadron Experimental Facility (HEF) is designed to handle intense slow-extraction proton beam from 30-GeV Main Ring (MR) of Japan Proton Accelerator Research Complex (J-PARC). A total amount of $3.6E19$ protons in the 2018 run were irradiated on the production target in HEF. In order to evaluate soundness of the production target, we have analysed long-term variation of temperature rise on the target, which can be affected by beam conditions. Predicted temperature rise measured with thermocouples mounted on the target was calculated from the existing training data of beam intensity, spill length (duration of beam extraction in 5.2 second accelerator cycle), and beam position on the target, using a linear regression analysis with a machine learning library, scikit-learn. As a result, predicted temperature rise shows good agreement with the measured one. We have also examined whether the present method of the predicted temperature rise from the existing training data can be applied to the new data in the future runs. The present paper reports the current status of the measurement system of temperature rise on the target with machine learning in detail.

INTRODUCTION

Hadron Experimental Facility [1] (HEF) at Japan Particle Accelerator Research Complex (J-PARC), shown in Figure 1, is designed to handle intense slow-extraction proton beam from 30-GeV Main Ring (MR). The period of beam extraction from MR to HEF is 2 seconds and the operation cycle is 5.2 seconds.

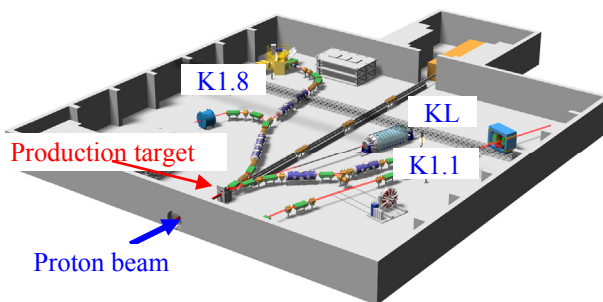


Figure 1: An illustration of the HEF.

Production Target

The production target [2], currently using at the HEF, is made of a gold and a copper block with coolant stainless pipes, as shown in the Figure 2. Gold is chosen for high density, high thermal conductivity, and good chemical stability. The current target is designed to be capable for up to 50-kW proton beams. The dimension of gold target is $15^W \times 6^H \times 66^L$ [mm]. The gold target is divided into 6 blocks in order to reduce thermal stress by beam irradiation. A double-headed design enables to switch the one target to the other quickly and remotely on demand. The water coolant pipes, embedded in the copper block, are made of stainless steel to avoid erosion and corrosion. The gold target, the copper block, and the coolant pipes are bonded with a Hot Isostatic Pressing (HIP) process. The production target is enclosed with an airtight chamber filled with circulating helium gas. The beam entry and exit are covered with beam windows.

In order to monitor temperature rise of the target, six thermocouples, named as TC1 to TC6, are mounted on top of each gold block along the beam direction. We also monitor temperatures of the copper block, the water and helium gas pipes, and the edge of the beam windows.

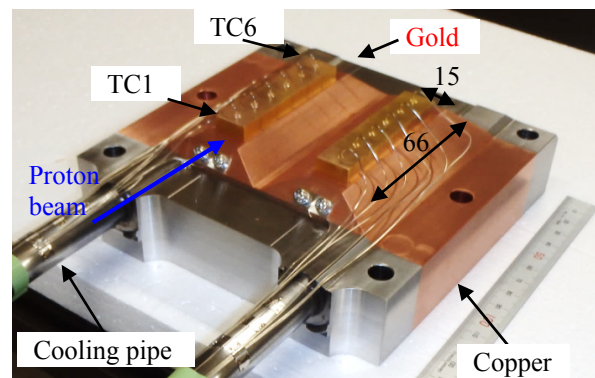


Figure 2: A photograph of production target.

During continuous 50 kW beam operation, temperature on the target rise close to 342K, the allowable limit estimated by a FEM stress analysis. In the point of soundness of the target, unexpected temperature rise by cumulative damage on the target may occur during a normal beam operation. Thus, it is important for damage control of the target to distinguish an unexpected temperature rise by damage from a normal drift due to fluctuation of beam conditions.

Recently, a number of machine-learning methods has been widely used in a variety of fields, and many easy-to-

[†]agari@post.kek.jp

use libraries, such as scikit-learn, becomes popular. We have adopted a machine-learning method to calculate temperature rise predicted from existing training data of various beam conditions, and compared to those measured with real-time data. If a difference between measured and predicted temperature rise becomes significantly larger than usual, it may indicate that an unexpected temperature rise occurred by a sudden decrease of thermal conductivity between gold and copper blocks. In addition, it would be helpful to construct a warning system using predicted temperature with more intense beam in future.

The requirements with the linear regression analysis are as follows:

- The required accuracy between measured and predicted temperature rise is sufficiently smaller than the margin between the nominal and the allowable temperature on the gold blocks. According to the data during the 2018 run, the difference between the allowable limit of temperature rise (342K) and the average temperature rise (321K) was 21K, 6.5% of the average temperature rise. Therefore, 1% of accuracy on predicted temperature should be sufficient.
- The required accuracy should be stable during at least one beam time lasting for a few months in order to use the predicted temperature as a signal for warning/intrlock system.

Monitoring Device

The current monitoring device is based on Programmable Logic Controller (PLC) with a Linux-CPU working as an embedded EPICS IOC on Yokogawa's FA-M3 PLC platform [3]. Temperature of the gold target, the copper block, and cooling water are monitored with thermocouple measuring devices (F3CX04-0N) with 100 milliseconds sampling rate. Sampled data are stored in the data registers on a sequence-CPU, and an EPICS-IOC, running on the adjoint CPU module, can simultaneously take data from the sequence CPU via shared memory. The start and stop timing of temperature measurement are synchronized to beam extraction time, using an on-beam gate signal distributed from the accelerator timing control system. The system of the monitoring PLC is shown in Figure 3 and Table 1. The monitored data are displayed graphically on the screens in the control room, and stored with a standard EPICS channel archiver [4] for data analysis.

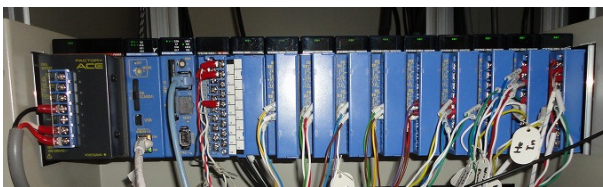


Figure 3: Photograph and illustration of the PLC.

Table 1: Module List of the PLC

Module	Model number
Sequence CPU	F3SP71-4S
Linux CPU	F3RP71-2L
A/D	F3AD04-0R
D/A	F3DA04-0N
Temperature monitoring	F3CX04-0N

ANALYSIS OF TEMPERATURE RISE WITH MACHINE LEARNING

Linear Regression Analysis

In order to calculate predicted temperature rise, shot-by-shot data during a certain period of beam time have been used as training data for machine learning. Temperature rise on the production target depends dominantly on beam intensity, spill length (duration of beam extraction), and horizontal and vertical beam positions. Therefore, predicted temperature rise is supposed to be expressed as a linear function of these four parameters, shown in the equation (1). A linear regression analysis with an open-source Python library, scikit-learn [5], has been used for the present analysis.

$$T = \alpha I_{beam} + \beta \frac{1}{S} + \gamma X + \delta Y + \epsilon \quad (1)$$

where T is the predicted temperature rise, I_{beam} is the beam intensity, S is the spill length, X is the horizontal beam position, Y is the vertical beam position. α , β , γ and δ are optimization coefficients, and ϵ is an intercept. The spill length is incorporated as a reciprocal because a shorter beam length gives higher temperature rise with a fixed intensity. Beam intensity and positions are measured with a DC-Current Transformer (DCCT) in the Main Ring and a Residual Gas Ionization Profile Monitor (RGIPM) [6] installed at about 1 m upstream of the production target, respectively.

We have evaluated accuracy of predicted temperature rise with the linear regression analysis with an indicator, so called ‘‘coefficient of determination’’. Coefficient of determination is given by the equation (2),

$$R^2 = 1 - \frac{\sum_i (y_i - f_i)^2}{\sum_i (y_i - \bar{y})^2} \quad (2)$$

where R is the coefficient of determination, y is the measured temperature rise, \bar{y} is the average of measured data in a beam period, and f is the predicted one.

RESULTS AND DISCUSSIONS

At first, we have calculated predicted temperature rise with the existing training data from January 27th to February 26th and those from June 2nd to 30th in 2018 in linear regression analysis.

When a continuous beam operation suspends due to machine failures and/or warnings issued by the instruments in the accelerator and beam-lines. Temperature of the production target drops down to that of the cooling water. After restart of continuous beam operation, it takes several shots of beam to resume nominal temperature on the target. In

Content from this work may be used under the terms of the CC BY 3.0 licence (© 2019). Any distribution of this work must maintain attribution to the author(s), title of the work, publisher, and DOI.

order to avoid uncertainty in the analysis, every first 3 shots just after resuming beam operation have been eliminated from sampled data in the present analysis.

Figure 4 shows a typical chart of temperature rise of TC4, which shows the maximum temperature rise among the six thermocouples on the gold blocks. A large shift on February 2nd in the chart is due to an artificial adjustment of spill length from 1.8 to 2.1 seconds in order to decrease the peak temperature on the target. Figure 5 shows a 1-D projection of Figure 4, and Table 2 indicates statistical means and standard deviations of 1-D projected distribution on each thermocouple (TC1-6). The statistical means are also expressed in percentage divided by the average temperature rise. All of mean value are within 0.2% of the averaged data, and fulfils our requirements.

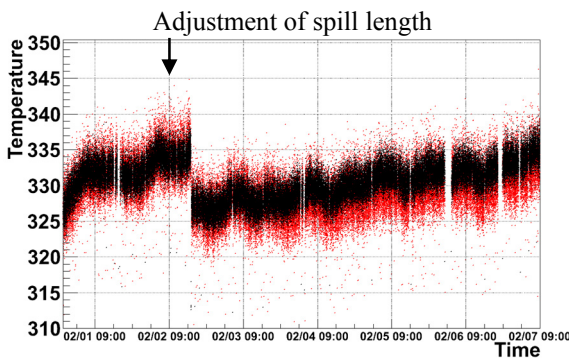


Figure 4: A typical chart of measured and predicted temperature rise of TC4 from January 31th to February 7th in 2018. Red and black point are measured and predicted temperature rise [K], respectively.

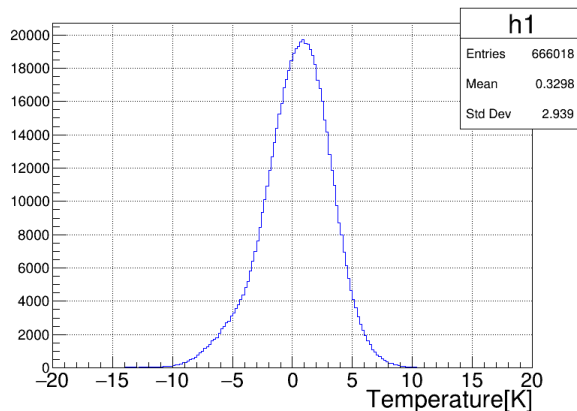


Figure 5: An 1-D projection of the difference between measured and predicted temperature rise in the 2018 run.

Table 2: Summary of 1-D Projections of All Thermocouples

Name	Mean		Standard deviation[K]
	[K]	[%]	
TC1	0.09	0.07	0.92
TC2	-0.42	0.17	1.66
TC3	-0.07	0.02	2.44
TC4	0.33	0.10	2.94
TC5	-0.05	0.02	2.02
TC6	-0.39	0.14	1.99

To improve coefficient of determination, we have also examined to incorporate the temperature rise of TC1 to the present linear regression analysis. Figure 6 shows that adding the TC1 data improves coefficient of determination by about 7%.

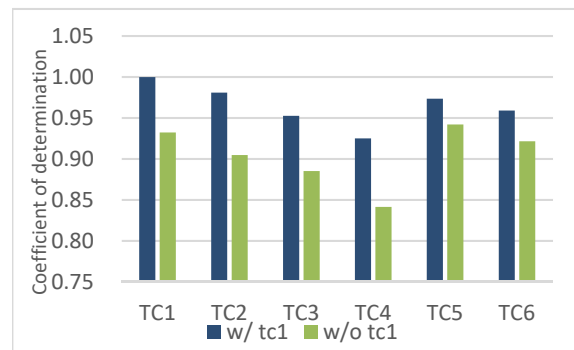


Figure 6: A bar chart of coefficient of determination. Blue and green bars are coefficient of determination calculated from the data with and without adding temperature rise of TC1, respectively.

The statistical means and standard deviations of the analysed data are summarized in Figure 7. Both means and standard deviations on all thermocouples have been improved by adding the TC1 data. The present result may indicate that TC1 would represent more precise information about the total amount of heat-deposit on the target rather than that provided by the beam intensity monitor. In the following results, TC1 data are always included in the linear regression analysis.

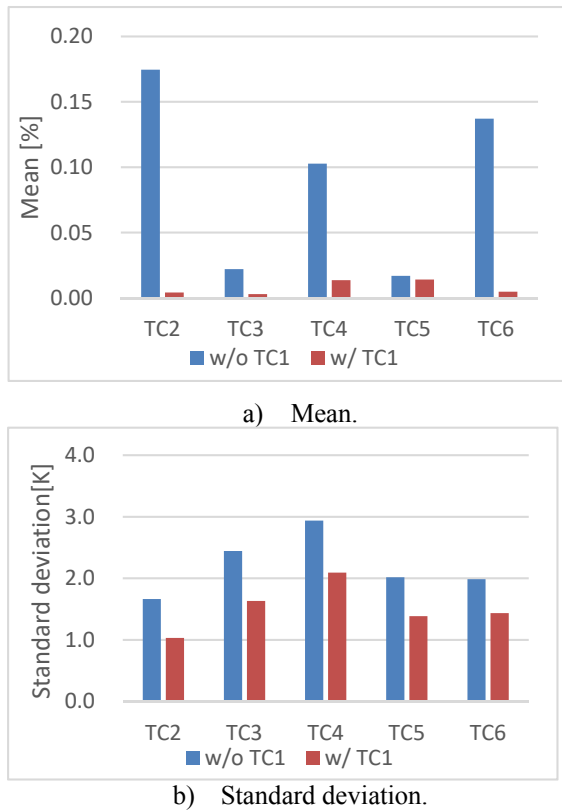


Figure 7: Bar charts of statistical means and standard deviations on all thermocouples in the 2018 run. Predicted temperature rise is calculated from the training data with TC1.

Generalization Performance

We have also studied whether the present method can be applied to unknown data in the future runs, so called as generalization performance. We have investigated two methods as follows:

- A) Applying the function evaluated by the training data in a certain beam operation to the fresh data obtained in the next.
- B) Applying the function evaluated by the training data accumulated during several hours at the beginning of a certain beam operation to the new data obtained in the remaining beam operation.

The training data of the linear regression analysis using both methods are comprised of beam intensity, spill length, beam positions and temperature rise of TC1.

In the method A), the function evaluated by the existing training data in the 2018 run has been applied to the fresh data from February 11th to March 18th in 2019.

Figure 8 shows a typical chart on TC3, and Table 3 indicates statistical means and standard deviations of all thermocouples. Predicted temperature rise is not in good agreement with the measured one, especially on TC3, 4 and 6. It might result from different beam optical and parameters of the accelerators between the 2018 and 2019 run.

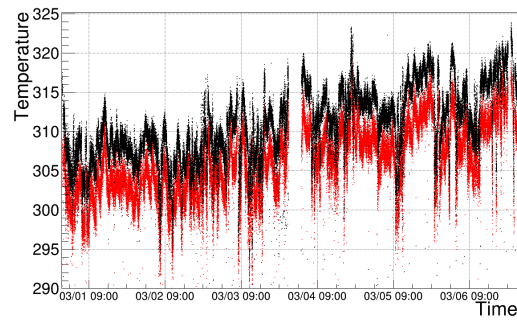


Figure 8: A typical chart of measured and predicted temperature rise of TC3 from March 1st to 7th in 2019. Black point is measured temperature rise. Red point is predicted temperature rise calculated from the training data in the 2018 run.

Table 3: Summary of 1-D Projections.

Name	Mean		Standard deviation[K]
	[K]	[%]	
TC2	0.90	0.39	0.99
TC3	-7.09	2.33	2.53
TC4	5.97	1.84	3.14
TC5	2.46	0.82	2.68
TC6	6.00	2.14	2.59

In the method B), the function evaluated by the training data accumulated for 0.5 - 12 hours from the beginning of the beam operation on March 1st in 2019 has been applied to the data obtained until March to 7th. Table 4 shows the duration and the number of the training data.

Table 4: Duration and Number of Training Data.

Duration [hours]	Number of data
0.5	94
1	440
2	1104
3	1732
6	3791
12	7776

Figure 9 shows a scatter plot of coefficient of determination and the number of the training data. The larger number of the training data gives the better Coefficient of determination.

Figure 10 shows a typical chart on TC3. Accuracy of predicted temperature rise has been improved, compared to Figure 9.

Content from this work may be used under the terms of the CC BY 3.0 licence (© 2019). Any distribution of this work must maintain attribution to the author(s), title of the work, publisher, and DOI.

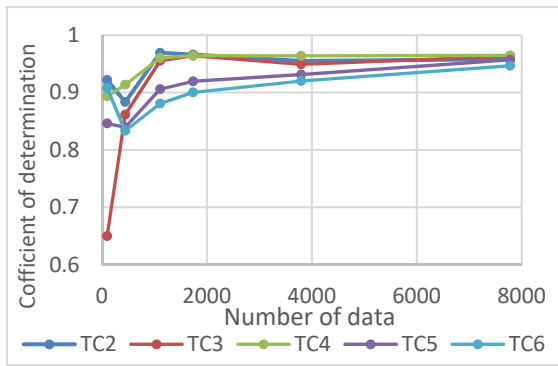


Figure 9: A scatter plot indicating coefficient of determination and the number of data. Horizontal and vertical axes are the number of data and coefficient of determination, respectively.

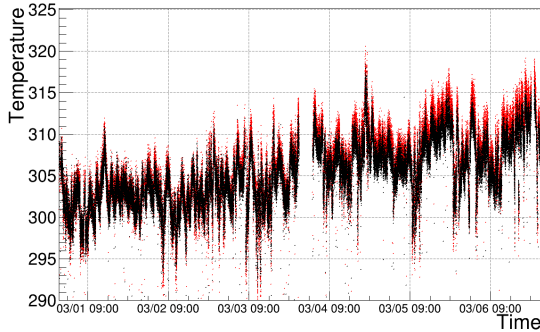
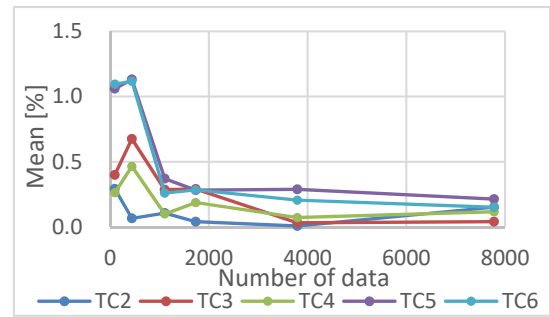
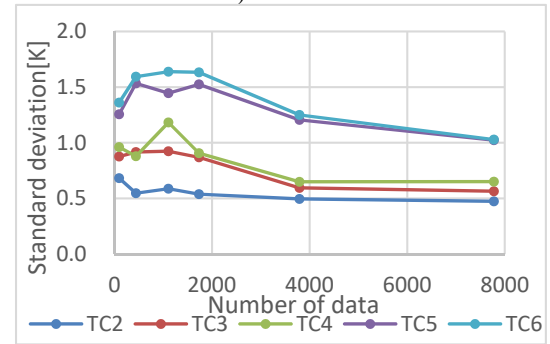


Figure 10: A typical chart of measured and predicted temperature rise of TC3 from 1st to 7th in March 2019. Black point is measured temperature rise. Red point is predicted temperature rise [K] calculated from the data for 2 hours just after the start of beam operation.

The statistical means and standard deviations of 1-D projected data are summarized in Figure 11. Means and standard deviations have been improved as the number of the training data increases. The result shows accumulating more than 3000 data as a set of training data would be sufficient for the analysis in the method B). The present comparison shows that the method B) works better than the method A), and the result suggests that we should accumulate data for more than 6 hours. However, we also prepare predicted temperature rise with the method A) for any contingency.



a) Mean.



b) Standard deviation.

Figure 11: Scatter plots of statistical means and standard deviations as increasing number of the data points in 2019. Horizontal axis is the number of training data.

CONCLUDING REMARKS

A Python machine learning library, scikit-learn, has been applied to evaluate a function of predicted temperature rise on the production target for damage control, using accumulated data of beam intensity, positions, spill length, and the TC1 thermocouple. Predicted temperature rise shows good agreement with measured one in the 2018 run.

The function of predicted temperature rise evaluated by the data accumulated for more than 6 hours at the beginning of a beam period could be applicable to predict the unexpected temperature rise in the remaining beam operation.

REFERENCES

- [1] K. Agari *et al.*, "Secondary charged beam lines at the J-PARC hadron experimental hall", *Progress of Theoretical and Experimental Physics (PTEP)*, 2012.
- [2] H. Takahashi *et al.*, "Indirectly water-cooled production target at J-PARC hadron facility", *J. Radioanalytical and Nuclear Chemistry*, Sept. 2015, vol. 305, no. 3, pp. 803-809.
- [3] EPICS Device and Driver Support for Yokogawa's F3RP71/61, <https://www-linac.kek.jp/cont/epics/f3rp61/>
- [4] EPICS Channel archiver, <https://ics-web.sns.ornl.gov/kasemir/archiver/>
- [5] Scikit-learn: machine learning in Python, <https://scikit-learn.org/stable/>
- [6] Y. Sato *et al.*, "Development of Residual Gas Ionization Profile Monitor for High Intensity Proton Beams", *IEEE Nuclear Science Symposium Conf.*, Puerto Rico, Oct. 2005, pp. 1043-1046.